# Beyond Fast Frequency Response: How Fast-Acting Energy Storage Suppresses Ultra-Low-Frequency Oscillations

1st Weike Mo
*Energy Electricity Research Center*
*Jinan University*
Zhuhai, Guangdong, China

2nd Qingqin Ma
*Energy Electricity Research Center*
*Jinan University*
Zhuhai, Guangdong, China

3rd Weicheng Lu
*School of Electric Power Engineering*
*South China University of Technology*
Guangzhou, Guangdong, China

4th Yingqi Liang
*China Southern Power Grid Co., Ltd.*
Guangzhou, China

5th Changsheng He
*Yunnan Electric Test&Research Institute (Group) Co.,Ltd*
Kunming, China

6th Yiping Chen*
*China Southern Power Grid Co., Ltd.*
Guangzhou, China
chenyiping@csg.cn

***Abstract*—Ultra-low-frequency oscillations (ULFO) below 0.1 Hz have become a serious stability concern in hydropower-dominated and low-inertia systems. This paper shows that fast-acting energy storage systems (ESS), originally installed for fast frequency response (FFR), can also provide effective damping for ULFO. Building on this insight, we develop a state-space framework that embeds ESS frequency-control loops and analytically clarifies how ESS capacity, control gains, and siting reshape ULFO modes. Eigenvalue loci with increasing ESS participation confirm a shift from weak or negative to positive damping. Time-domain simulations on a representative hydropower-dominated network reproduce a historical-type ULFO event and demonstrate that suitably sized and sited ESS units suppress oscillations without wholesale governor retuning; with ESS support, only a subset of governors requires adjustment to meet damping targets. Overall, ESS markedly reduces oscillation amplitude, increases damping in the ULFO band, and remains effective across high-renewables scenarios, offering a practical complement to governor-centric solutions.**

***Index Terms*—Ultra-low-frequency oscillations, energy storage, auxiliary damping, eigenvalue analysis.**

## I. Introduction

The rising share of clean energy has heightened the risk of ULFO in hydropower-dominated systems with large outbound transfers. Observed in regions such as Yunnan/Sichuan (China), Colombia, and Ireland, ULFO appears as a grid-wide synchronous frequency swing, driving large fluctuations in frequency and power flow. Consequences range from equipment wear and HVDC blocking to frequency collapse, posing serious threats to secure operation. Understanding ULFO mechanisms and developing effective countermeasures is therefore essential for high-renewables power systems.

ULFO stems from negative damping arising from the interaction between turbine water-hammer dynamics and governor control, which sustains a mismatch between mechanical and electromagnetic power. Existing mitigation follows two main tracks: governor parameter optimization and auxiliary damping control.

For parameter optimization, [1], [2] address single-machine cases using improved beetle antennae search and PSO to tune PID gains, while [3] proposes deep reinforcement learning for hydropower clusters. By building an analytical damping model with security constraints, the model balances oscillation suppression and frequency-regulation performance. To adapt online, [4] designs a switching-type governor based on local damping contribution ratios.

For auxiliary damping, [5] optimizes an SVC-based controller; [6], [7] add active-power damping support from PV plants. Governor-based designs show that traditional PSS offers limited damping in the ULFO band, whereas a governor-based PSS (GPSS) can supply significant positive damping [8]. A proportional–resonant PSS (PR-PSS) is proposed in [9], with DRL used to retune parameters across operating points. Further, the control-frame-based GPSS (CFSGPSS) in [10] sustains ULFO suppression and improves PFR relative to PID tuning.

However, optimizing governor parameters can blunt fast unit response and degrade PFR, slowing post-fault recovery. Added damping loops may also compromise performance at other frequencies (e.g., inter-area/low-frequency modes). Meanwhile, higher penetrations of wind and PV intensify frequency variability, increasing demands on hydropower regulation and potentially aggravating ULFO risk.

To overcome these limitations, this paper shifts the focus to ESS with millisecond-level response and examines the mechanisms by which ESS participation in FR shapes ULFO modes. The detailed contributions are as follows: 1) clarifies how millisecond-response ESS participation in FR reshapes ULFO modes, relieving the regulation burden on hydropower

This work is supported by the National Key Research and Development Program of China (Key technologies on intelligent dispatch of power grid under 20% new energy integration scenario, No. 2022YFB2403503).

979-8-3315-8138-1

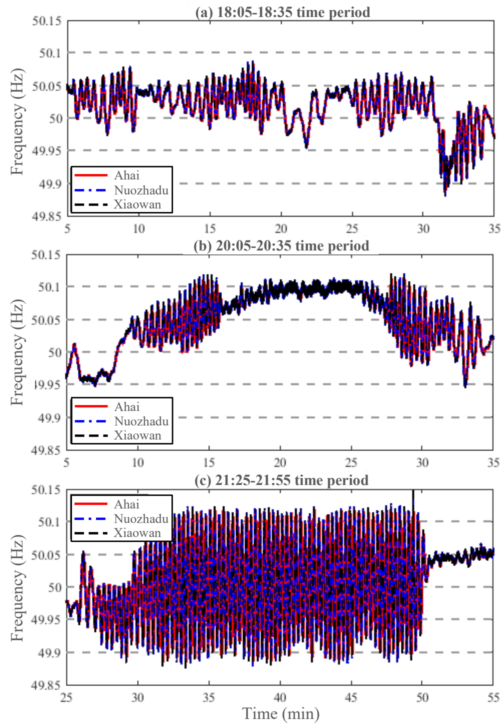


Fig. 1. The frequency of different power plants.

units and enhancing system damping; 2) develops a detailed multi-machine model with ESS frequency-control loops to analyze the impacts of ESS capacity, control parameters, and interconnection location on dominant ULFO modes; 3) demonstrates that properly configured ESS can suppress oscillation amplitude, increase damping in the ultra-low-frequency band, and remain effective under high-renewables scenarios.

## II. Review of Ultra-Low-Frequency Oscillation

### A. ULFO in Yunnan Asynchronous Power Grid

The China Southern Power Grid (CSG) planned Yunnan as a separate sending-end system tied to the main grid via six back-to-back HVDC links. During an asynchronous interconnection test on March 28, 2016, after AC tie-line disconnection, the Yunnan grid exhibited multi-hour frequency swings: around 50.05/49.95 Hz during up/down regulation, intensifying to 0.053 Hz between 21:00–22:00 (as shown in Fig. 1).

Disabling Automatic Generation Control (AGC) or reducing output was ineffective; the oscillation ceased only after disabling primary frequency control at six major hydropower stations.

### B. Phenomenology

ULFO is a phenomenon characterized by frequency stability, in which generators remain synchronized and exhibit nearly identical trajectories across the grid within a frequency band of less than 0.1 Hz. This behavior is distinct from conventional low-frequency oscillations, which occur between 0.2 and 2 Hz and are driven by relative rotor-angle motions. The 0.053 Hz oscillation observed during the 2016 Yunnan event confirms the frequency nature of this phenomenon.

### C. Mechanism

In hydro-dominant systems, hydraulic inertia from the water-hammer effect and governor phase lag can inject negative damping in the ULFO band if PID gains are poorly tuned, undermining small-signal stability [11], [12]. Weak system connectivity further lowers the oscillation frequency and damping ratio as hydro share rises, aggravating ULFO risk [13].

### D. The Current Measures of Yunnan Power Grid to Deal with ULFO and Its Limitations

Currently, engineering practice emphasizes governor-parameter optimization, which has removed ULFO under multiple fault scenarios. However, optimization entails trade-offs and parameter uncertainty: it can blunt fast response and PFR, and depends on hard-to-generalize parameters such as the water-hammer time constant $T_w$, limiting achievable damping margins.

## III. Analysis of the Change of Frequency Characteristic in Yunnan Asynchronous Power Grid

### A. Large-scale Grid Connection of Renewable Energy Sources

Since 2021, the Yunnan asynchronous system has changed in two material ways:

1) Large-scale wind and PV integration has reduced inertia and available frequency-regulation resources, while ULFO has further weakened hydro units' effective regulation capability; together, these factors increase frequency instability risk.
2) In parallel, the rapid deployment of new-type ESS has improved system regulation speed and flexibility; by July 2025, cumulative ESS capacity in Yunnan reached **5,465.4 MW**, ranking first in CSG and among the top nationwide. This development offers a practical path to supply the missing damping at ultra-low frequencies.

Therefore, the rapid development of energy storage technologies offers a promising path to provide the missing damping.

### B. New Type of Energy Storage Participates in FR - Damping Enhancement Mechanism

The participation of energy storage in FR delivers direct frequency support through rapid power response. The steady-state power equation of the ESS is as follows:

$$(f_{\text{ref}} - f) + b_p(P_{\text{ref}} - P_{\text{ESS}}) = 0 \tag{1}$$

Thus, the ESS equipped with droop-based active-power control provides fast frequency support:

$$P_{\text{ESS}} - P_{\text{ref}} = -\frac{1}{b_p}(f - f_{\text{ref}}) \tag{2}$$

979-8-3315-8138-1

Recorded as:

$$\Delta P_{\text{ESS}} = -\frac{1}{b_p}\Delta f \tag{3}$$

Among which $\Delta P_{\text{ESS}} = P_{\text{ESS}} - P_{\text{ref}}, \Delta f = f - f_{\text{ref}}$. When the grid frequency rises, the ESS absorbs power; when it falls, it injects power, creating an immediate positive-damping effect. Because its response is nearly delay-free (millisecond-level), the ESS behaves as an additional damping term in the system swing equation:

$$T_J\frac{df}{dt} = P_m^* - P_e^* - D_{\text{syn}}\Delta f + \Delta P_{\text{ESS}} = P_m^* - P_e^* - (D_{\text{syn}} + \frac{1}{b_p})\Delta f \tag{4}$$

That is:

$$T_J\frac{df}{dt} = P_m^* - P_e^* - D_{\text{eq}}\Delta f \tag{5}$$

where $T_J$ is the system inertia constant (in seconds), $D_{\text{eq}} = D_{\text{syn}} + D_{\text{ESS}} = D_{\text{syn}} + \frac{1}{b_p}$. Hence, ESS participation increases total damping and improves the real part of the dominant eigenvalue.

## IV. The Establishment of the System State Equation and ASF Model Considering Energy Storage

Given the millisecond-scale response of ESS, droop control is effectively delay- and hysteresis-free at ULFO time scales, i.e., it manifests as an additional damping term in the equivalent generator. We therefore adopt an ASF (Fig. 2)/state-space formulation to quantify how ESS capacity and controller gains shift the dominant eigenvalues toward the left half-plane.

The hydro-turbine governor, ESS, and synchronous generator dynamics are written as (6)∼(11), and assembled into the compact state-space form $T\frac{dx}{dt} = Jx$ in (12). This yields a transparent mapping from $[\alpha, K_P, K_I, b_p2]$ and $[T_g, T_p, T_d, T_w, b_p, b_t]$ to the ULFO eigenstructure.

Here, $T_J$ represents the inertia time constant of the system equivalent generator, $D_{\text{syn}}$ denotes the system damping coefficient (excluding ESS); In the energy storage system, $K_P$ and $K_I$ are proportional and integral gains, respectively; and $b_p2$ is the droop coefficient. In the governor, $T_g$ is the servo time constant; $b_p$ represents the permanent droop coefficient, $T_p$ denotes the pilot valve and servomotor time constant, $T_d$ is the dashpot time constant, $T_w$ represents the water hammer effect time constant, and $b_t$ indicates the transient droop ratio. and $\alpha \in [0, 1]$ represents the energy storage penetration level.

Hydro-turbine governor equation:

$$T_gT_p\frac{dx_1}{dt} = -(1-\alpha)x_6 - b_px_2 - x_4 - T_gx_1 \tag{6}$$

$$\frac{dx_2}{dt} = x_1 \tag{7}$$

$$T_d\frac{dx_4}{dt} - b_tT_d\frac{dx_2}{dt} = -x_4 \tag{8}$$

$$0.5T_w\frac{dx_5}{dt} + T_w\frac{dx_2}{dt} = x_2 - x_5 \tag{9}$$

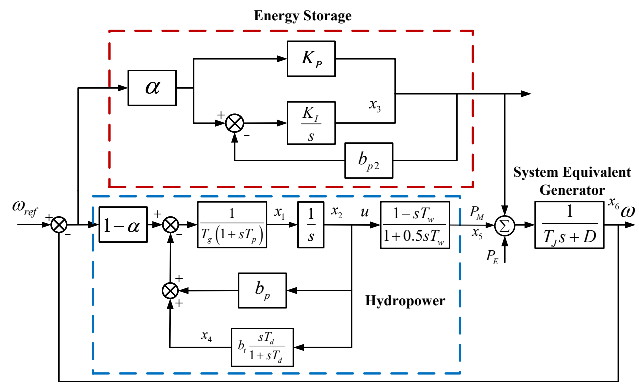


Fig. 2. The ASF model diagram of the hydropower system with energy storage.

Energy storage system equations:

$$\frac{dx_3}{dt} = -\alpha K_Ix_6 - b_{p2}K_I(x_3 - \alpha K_Px_6) \tag{10}$$

Synchronous generator equations:

$$T_J\frac{dx_6}{dt} = x_5 + x_3 - \alpha K_Px_6 - D_{\text{syn}}x_6 \tag{11}$$

The state equations of the complete system are formulated as follows:

$$T\frac{dx}{dt} = Jx \tag{12}$$

where the coefficient matrix $T$ is given by:

$$\begin{pmatrix} T_gT_p & & & & & \\ & 1 & & & & \\ & & 1 & & & \\ & & -b_tT_d & T_d & & \\ & & T_w & & 0.5T_w & \\ & & & & & T_J \end{pmatrix}$$

and the Jacobian matrix $J$ is:

$$\begin{pmatrix} -T_g & -b_p & & -1 & & \alpha-1 \\ 1 & & & & & \\ & & -b_{p2}K_I & & -\alpha K_I(1-b_{p2}K_P) & \\ & & & -1 & & \\ & 1 & & & -1 & \\ & & 1 & & 1 & -\alpha K_P - D_{\text{syn}} \end{pmatrix}$$

## V. Case Study

### A. Case Study Based on the ASF Model

The parameter setting in simulations is listed in Table V-A, and the initial ESS share $\alpha$ is set to 0.

Without ESS integrated into the system, the system eigenvalues are shown in Fig. 3(a). The system exhibits a pair of negatively damped oscillatory modes at $0.034 \pm 0.229i$, with an oscillation frequency of approximately 0.0364 Hz, which falls within the ULFO range.

With the increase in the energy storage ratio $\alpha$, the damping ratio of the ULFO mode (Eigenvalue 3 in the figure below) improves from a negative value to a positive one, as seen in the root-locus trajectory (Fig. 3 (b)).

979-8-3315-8138-1

TABLE I
PARAMETERS AND VALUES

| Parameter | Value | Parameter | Value |
|---|---|---|---|
| $T_J$ | 10 s | $b_p$ | 0.05 |
| $D$ | 1 | $T_p$ | 0.04 s |
| $K_P$ | 10 | $T_d$ | 5 s |
| $K_I$ | 3 | $T_w$ | 5 s |
| $b_{p2}$ | 0.005 | $b_t$ | 0.5 |
| $T_g$ | 0.25 s | | |

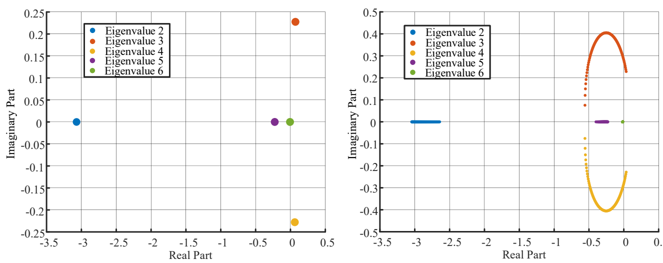

(a) System eigenvalue distribution (b) System eigenvalue trajectory

Fig. 3. The system eigenvalue and eigenvalue trajectory.

Thus, investing a certain proportion of energy storage in system FR enhances the damping ratio in the ULFO mode. Therefore, while ensuring a sufficient damping ratio for the ULFO mode, it is feasible to appropriately relax the FR pressure of hydroelectric units to maintain system frequency stability under large disturbances.

### *B. Case Study Based on Yunnan Power Grid Data*

*1) Reproduction of the ULFO Phenomenon:* A time-domain simulation was conducted using the bulk power analysis (BPA) software, based on operational data from the Yunnan power grid with a high penetration of renewable energy sources. The water hammer time constants $T_w$ for the Nuozhadu Plant and 12 other plants were set to measured values, while the governor PID parameters were maintained at their original settings (i.e., unoptimized for ULFO mitigation). The dead band of the HVDC Frequency Limit Controller (FLC) was set to ±0.15 Hz.

The disconnection of one unit at the Xiaowan Plant was simulated as a large power disturbance. The system subsequently exhibited ULFO with an amplitude of approximately ±0.15 Hz and an oscillation period of 18 seconds. The power output of the major hydroelectric plants varied in phase with the system frequency. The HVDC FLC, operating outside its dead band, also adjusted its power in phase with the frequency, thereby containing the frequency deviation within the ±0.15 Hz range (Fig. 4).

*2) ESS Configuration:* ESS1, ESS2, ESS3, and ESS4 are nodal energy storage systems situated at specific locations within the Yunnan power grid. Four nodal ESS units are modeled with field-calibrated parameters: ESS1 (166 MW), ESS2 (134 MW), ESS3 (166 MW), and ESS4 (134 MW), battery rack rated power 1.25 MW, initial State of Charge

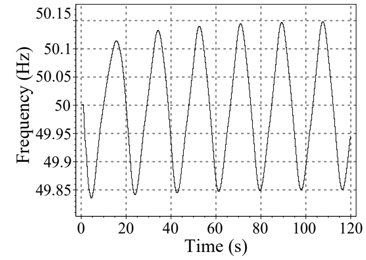


Fig. 4. The reproduction result of ULFO in Yunnan power grid.

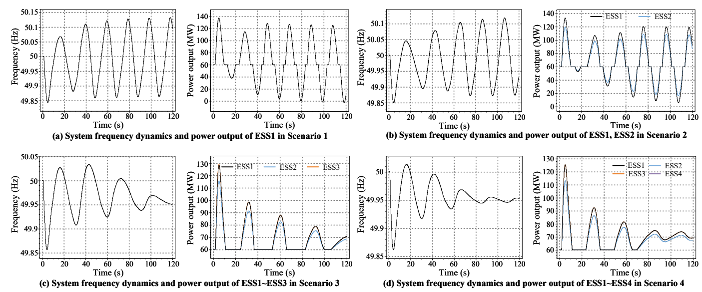


Fig. 5. Scenarios 1–4: frequency response and ESS power; ULFO amplitude shrinks as the participation number of ESS units increases.

(SOC) of 0.5, frequency deviation dead band of ±0.033 Hz, and a frequency regulation droop coefficient of 200.

*3) Analysis of the Suppression Effect of ESS on ULFO in Different FR Capacities:* The influence of energy storage-based FR on the ULFO mode was validated under scenarios of integrating 1 to 4 energy storage units:

Scenario 1: Only ESS1 participates in FR.

Scenario 2: Only ESS1 and ESS2 participate in FR.

Scenario 3: ESS1, ESS2, and ESS3 participate in FR.

Scenario 4: ESS1, ESS2, ESS3, and ESS4 integrated for FR.

As shown in Fig. 5, the integration of four 150 MW energy storage units for FR control can suppress the occurrence of ULFO without modifying the governor parameters of the hydroelectric units.

*4) Optimizing Governor Parameters of Selected Hydropower Plants with FR participation of ESS:* Furthermore, to analyze the impact of energy storage-assisted frequency regulation on relaxing the frequency regulation requirements for hydroelectric units, the governor parameters of the hydropower station units are listed in Table II. were optimized using the ULFO suppression method. Simultaneously, simulation analyses were conducted to assess the impact of different numbers of energy storage units on frequency regulation.

TABLE II
GOVERNOR OPTIMIZATION PARAMETERS

| Power Plant | Unit | $K_P$ | $K_D$ | $K_I$ |
|---|---|---|---|---|
| Nuozhadu | #1∼#9 | 4.00 | 1.00 | 0.80 |
| Xiaowan | #1∼#6 | 3.79 | 1.90 | 0.76 |
| Jinanqiao | #1∼#4 | 4.42 | 2.21 | 0.88 |

979-8-3315-8138-1

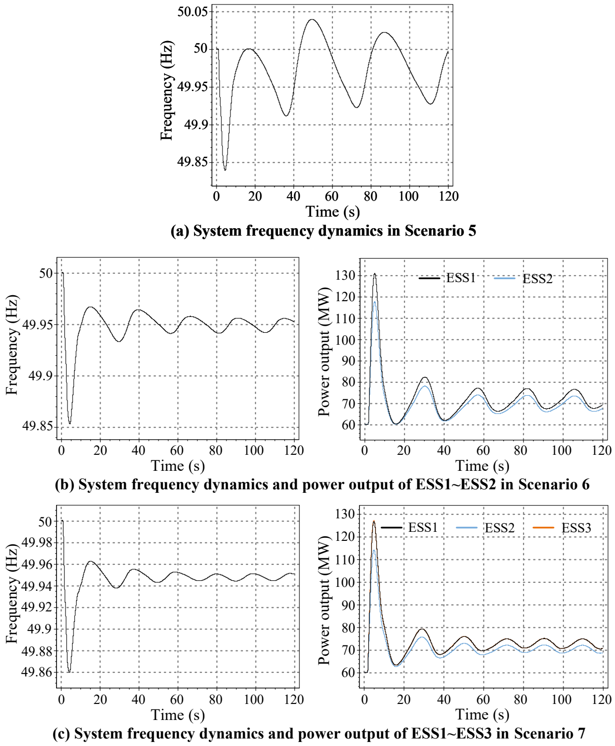

(a) System frequency dynamics in Scenario 5

(b) System frequency dynamics and power output of ESS1~ESS2 in Scenario 6

(c) System frequency dynamics and power output of ESS1~ESS3 in Scenario 7

Fig. 6. Scenarios 5–7: frequency response and ESS power; system damping improved by the optimization of the governor parameters and the collaborative effect of the participation of ESS in FR.

Scenario 5: No energy storage participates in frequency regulation.

Scenario 6: Only ESS1 and ESS2 participate in frequency regulation.

Scenario 7: ESS1, ESS2, and ESS3 participate in frequency regulation.

According to Fig. 6, with three 150-MW ESS participating in frequency regulation, only three hydropower plants require governor parameter optimization to meet damping targets.

Based on the comprehensive case studies, the participation of energy storage in frequency regulation alters the underlying mechanism of ULFO. Its rapid power response alleviates the frequency regulation burden on hydroelectric units. Simultaneously, through droop control, the energy storage injects power in opposition to frequency deviations, thereby introducing positive damping (with its magnitude proportional to the installed capacity) and consequently enhancing the system's damping characteristics. A properly configured energy storage system can effectively suppress oscillations, improve the ultra-low frequency damping ratio, and demonstrate strong adaptability even in scenarios with high penetration of renewable energy sources.

## VI. Conclusion

This paper establishes a mechanism-to-model-to-practice pathway for ESS-based suppression of ULFO in hydropower-dominated systems. Mechanistically, droop-controlled ESS provides near-instantaneous bidirectional power, manifesting as an added damping term in the swing equation and directly enhancing the damping ratio of the dominant ULFO mode. Analytically, the derived ASF/state-space model with embedded ESS loops explains how ESS capacity, controller gains, and penetration jointly shift eigenvalues into the left half-plane. Practical case studies calibrated to the Yunnan system show that integrating several 150-MW ESS units at suitable locations suppresses ULFO without exhaustive governor retuning; with ESS support, only a subset of hydro governors needs optimization to meet damping targets, easing FR pressure on hydropower units. Overall, ESS provides effective auxiliary damping, reduces oscillation amplitude, and preserves adaptability under high-renewables conditions—offering a scalable complement to governor-centric solutions for frequency stability in future hydro-rich grids.

## References


[1] J. Li, D. Yang *et al.*, "Optimal control strategy of turbine governor parameters based on improved beetle antennae search algorithm," *Tehnički vjesnik*, vol. 28, no. 4, pp. 1082–1090, 2021.

[2] W. Yan and Y. Sun, "Research on governor parameter optimization to suppress ultra-low frequency oscillation of power system caused by hydropower unit," in *Journal of Physics: Conference Series*, vol. 2087, no. 1. IOP Publishing, 2021, p. 012001.

[3] X. Lu *et al.*, "Correlating analysis and optimization between hydropower system parameters and multi-frequency oscillation characteristics," *ENERGY*, vol. 304, 2024.

[4] G. Cai *et al.*, "Suppression method of ultralow-frequency oscillation under ambient excitation in hydro-dominant power systems," *RENEWABLE ENERGY*, vol. 223, 2024.

[5] H. Shi *et al.*, "An optimized additional damping control for suppressing ultra-low frequency oscillation based on SVC," *IET Renewable Power Generation*, vol. 18, no. 14, pp. 2238–2247, 2024.

[6] S. Wang *et al.*, "Ultra-low frequency oscillation damping control method for hydro-photovoltaic integrated systems," *IEEE Transactions on Power Electronics*, vol. 40, no. 1, pp. 2397–2418, 2025.

[7] X. Zeng *et al.*, "A robust design method for ultra-low-frequency oscillation suppression control in hydro-photovoltaic complementary systems," *Applied Sciences-Basel*, vol. 13, no. 19, 2023.

[8] X. Shi, G. Ruan, H. Lu, H. Chen, W. Cai, H. Ron, G. Chen, and Y. Zhao, "Analysis of ultra-low frequency oscillation in hydro-dominant power system and suppression strategy by gpss," *IEEE Transactions on Industry Applications*, 2023.

[9] G. Zhang, W. Hu, D. Cao, Q. Huang, J. Yi, Z. Chen, and F. Blaabjerg, "Deep reinforcement learning-based approach for proportional resonance power system stabilizer to prevent ultra-low-frequency oscillations," *IEEE Transactions on Smart Grid*, vol. 11, no. 6, pp. 5260–5272, 2020.

[10] Y. Jia, B. Tan, W. Zhang, D. Jiang, C. Yang, and Y. Wen, "A novel control strategy for hydraulic turbines to consider both primary frequency regulation and ultra-low frequency oscillation suppression," *Energies*, vol. 17, no. 5, p. 1067, 2024.

[11] Y. Chen, Y. Liu, Z. Tang, J. Hou, Y. Zhang, W. Mo, and H. Chen, "Analysis of ultra-low frequency oscillation in yunnan asynchronous sending system," in *2017 IEEE Power & Energy Society General Meeting*. IEEE, 2017, pp. 1–5.

[12] W. Mo, Y. Chen, H. Chen, Y. Liu, Y. Zhang, J. Hou, Q. Gao, and C. Li, "Analysis and measures of ultralow-frequency oscillations in a large-scale hydropower transmission system," *IEEE Journal of Emerging and Selected Topics in Power Electronics*, vol. 6, no. 3, pp. 1077–1085, 2017.

[13] P. Wang, Q. Jiang, B. Li, T. Liu, X. Li, G. Chen, X. Zeng, and F. Blaabjerg, "Ultra-low frequency oscillation analysis considering thermal-hydro power proportion," *International Journal of Electrical Power & Energy Systems*, vol. 148, p. 108919, 2023.


979-8-3315-8138-1